Available online at www.sciencedirect.com
SCIENCE DIRECT
ELSEVIER
Polymer 47 (2006) 3591–3598
polymer
www.elsevier.com/locate/polymer

Microstructural studies on $BaCl_2$ doped poly(vinyl alcohol)

R.F. Bhajantri [a], V. Ravindrachary [a,*], A. Harisha [a], Vincent Crasta [c], Suresh P. Nayak [b], Boja Poojary [b]

[a] *Department of Physics, Mangalore University, Mangalagangotri, Mangalore 574 199, India*
[b] *Department of Chemistry, Mangalore University, Mangalagangotri, Mangalore 574 199, India*
[c] *Department of Physics, St Joseph Engineering College, Vamanjoor, Mangalore 575 028, India*

Received 7 October 2005; received in revised form 2 January 2006; accepted 17 March 2006

Abstract

We have studied the effect of $BaCl_2$ dopant on the optical and microstructural properties of a polymer poly(vinyl alcohol) (PVA). Pure and $BaCl_2$ doped PVA films were prepared using solvent casting method. These films were characterized using FTIR, UV–visible, XRD and DSC techniques. The observed peaks around 3425 cm^{-1}, at 1733 cm^{-1} and 1640 cm^{-1} in the FTIR spectra were assigned to O–H, C=C stretching and acetyle C=O group vibrations, respectively. In the doped PVA shift in these bands can be understood on the basis of intra/inter molecular hydrogen bonding with the adjacent OH group of PVA. The UV–visible spectra shows the absorption bands around 196 nm and shoulders around 208 nm with different absorption intensities for doped PVA, which are assigned to $n \rightarrow \pi^*$ transition. This indicates the presence of unsaturated bonds mainly in the tail–head of the polymer. Optical band energy gap is estimated using UV–visible spectra and it decreases with increasing dopant concentration. The powder XRD shows an increase in crystallinity in the doped PVA, which arises due to the interaction of dopant with PVA causing a molecular rearrangement within the amorphous phase of polymer. These modifications also influence the optical property of the doped polymer. The DSC study also supports increasing crystalline thickness and degree of crystallinity due to doping.

Keywords: Poly(vinyl alcohol); Polymer microstructure; Optical properties

1. Introduction

Polymeric materials have attracted the scientific and technological researchers, because of their wide applications. This is mainly due to the lightweight, good mechanical strength, optical properties and makes them to be multi-functional materials [1]. Moreover, these polymers are traditionally considered as an excellent host material for composites. In recent years, the doped polymers have been the subjects of interest for both theoretical and experimental studies, because of the physical and chemical properties needed for specific application may be obtained by adding or doping with some dopant. It is observed that doping a polymer with metal salts has significant effect on their physical properties including optical, thermal, electrical properties. These changes in physical properties, depends on the chemical nature of the dopant and the way in which they interact with the host polymer. Systematic investigations reported in literature shows that, many polymers have two coexistent phases, crystalline and amorphous. When such polymers are doped with suitable dopant, it may interact either in the amorphous fraction or in the crystalline fraction of the polymer and in both the cases polymeric property will alter. Hence, the complete information about the effect of additives on a specific polymer helps in tailoring that polymer for a particular application [2,3].

Poly(vinyl alcohol) (PVA) is a polymer that has been studied intensively due to its several interesting physical properties, which are useful in technical applications including biochemical and medical. The important feature of semicrystalline PVA is that the presence of crystalline and amorphous regions and its physical properties, which are resulting from the crystal–amorphous interfacial effects. These two regions are well separated by portions of an intermediate degree of ordering, which enhances the macromolecule, producing several crystalline and amorphous phases [2]. Recently, PVA films are doped with multiple valance metal ions and showed that a strong dependence of donor–acceptor mechanism between the metal ion and the polymer matrix. Various research groups have studied the optical, structural and other properties of PVA with different dopant like, I/KI, CuCl, ZnSe,

* Corresponding author. Tel.: +91 824 2287363; fax: +91 824 2287367.
E-mail address: vravi2000@yahoo.com (V. Ravindrachary).

0032-3861/$ - see front matter © 2006 Elsevier Ltd. All rights reserved.
doi:10.1016/j.polymer.2006.03.054

CdS, $NiCl_2$, $MnCl_2$, $MgBr_2$, CrF_3, $FeCl_3$, etc. using different techniques. These studies shows, the changes in the properties like crystallinity, structural and optical behavior, etc. of the polymer due to doping. PVA is normally a poor electric conductor; it can become conductive upon doping with some dopant. The small conducting nature of doped PVA is thought to be due to the high physical interactions between polymer chains and dopant via hydrogen bonding with hydroxyl groups as well as the complex formation [2–7].

The optical absorption spectroscopy (UV–visible, IR) is an established tool to investigate the effect of dopant on the microstructure of the polymer, particularly on the band structure and electronic properties including the energy gap E_g. Additions of the dopants to a polymer modify the energy band gap E_g, which depends on the type and magnitude of the defect concentration caused by the dopant. Hence, these modifications give information on the optical, electronic and microstructural behavior of the polymer. In addition, the change in the optical energy band gap E_g indicates the occurrence of local cross linking within amorphous phase of the polymer in such a way as to increase the degree of ordering in these parts [2]. The thermal analysis is another useful method to define a suitable processing condition for polymers. This provides useful guidelines for the applications as well as drawing information on thermal properties-polymer structure relationships. Differential scanning calorimetry (DSC) is a major tool to study the crystallization kinetics; thermal stability includes the glass transition and melting temperatures of polymers. The thermal treatment or thermal history of a semicrystalline polymer will be reflected in its melting behavior. For many semi-crystalline polymers, double and multiple melting peaks were observed in DSC scan and various interpretations were proposed for the origin of multiple melting peaks. Many authors have explained these double melting behavior using the melt–recrystallization model. This model suggests that the low-temperature and high-temperature peaks in the DSC melting curve are attributed to the melting of some amount of original crystals and to the melting of crystals formed through the melt–recrystallization process during a heating scan, respectively. The melting proceeds through the process of the melting of original crystals, recrystallization and melting of recrystallized and perfected crystals [8–10].

In view of this it is very important to note that the dopant modifies the structure of the polymer and hence its properties. Since, the change in polymer properties are mainly depends on the nature of the dopant and the way in which it interacts with the polymer, we have selected a divalent metal salt $BaCl_2$ as dopant for our study. The effect of this divalent dopant on the microstructural, optical and thermal properties of PVA was studied using FTIR, UV–visible, XRD and DSC techniques.

2. Experimental

2.1. Sample preparation and characterization

The PVA used in this work were obtained in powder form from M/s. s.d. fine-Chem. Ltd, Mumbai, has approximate molecular weight 125,000 and its degree of saponification is 86–89%. The PVA films with different amounts of $BaCl_2$ dopant were prepared by solution casting method. A known quantity of PVA powder was added to doubly distilled water and kept it for 48 h to swell the granules with stirring the solution at 40 °C for complete dissolution. Required quantity of $BaCl_2$ was also dissolved in doubly distilled water and added to the polymeric solution with continuous stirring. This solution was kept aside to get a suitable viscosity. The solution so obtained was poured on to a cleaned glass plate and dried at room temperature. After drying, the films were peeled from the plate and kept in vacuum desiccator for further study. The thickness of the films were in the range of 0.05–0.2 mm. PVA films doped with $BaCl_2$ mass fractions of 0, 1, 5, 10, and 20 M (wt%) were prepared by using the relation

$$M(\text{wt\%}) = \frac{m_d}{m_p + m_d} \times 100$$

where m_d and m_p are the weight of dopant and polymer, respectively.

Optical studies of the PVA, with and without $BaCl_2$ doped films were carried out using UV–visible and FTIR Spectrophotometers. The UV–visible spectra were recorded using SECOMAM ANTHELIE-284 UV–vis Spectrophotometer in the wavelength range 195–1000 nm and the infrared spectra were recorded using a SHIMADZU FTIR-8700 Spectrophotometer in the wave number range 400–4000 cm^{-1} with a resolution of 4 cm^{-1}.

The thermal analysis was performed using SIMADZU DSC-50 from room temperature to 195 °C at the heating rate of 10 °C/min. under nitrogen atmosphere.

The X-ray diffractograms of the samples were recorded using a Bruker D8 Advance X-ray diffractometer with Ni-filtered, Cu K_α radiation of wavelength $\lambda = 1.5406$ Å, with a graphite monochromator. The scan was taken in the 2θ range 2–50° with a scanning speed and step size of 1°/min and 0.01°, respectively.

3. Results and discussion

3.1. FTIR studies

The FTIR spectra of pure and $BaCl_2$ doped PVA samples were obtained using KBr pelleting method and the results are shown in the Fig. 1. Using FTIR spectra a strong broad band at 3425 cm^{-1} is assigned to O–H stretching vibration of hydroxyl groups of PVA. The band corresponding to C–H asymmetric stretching vibration occurs at 2928 and C–H symmetric stretching vibration at 2853 cm^{-1}. The bands at 1733 corresponds to C=C stretching vibration and 1640 cm^{-1} corresponds to an acetyle C=O group and can be explained on the basis of intra/inter molecular hydrogen bonding with the adjacent OH group. The sharp band at 1089 cm^{-1} corresponds to C–O stretching of acetyl group present on the PVA back bone. The corresponding bending, wagging of CH_2 vibrations

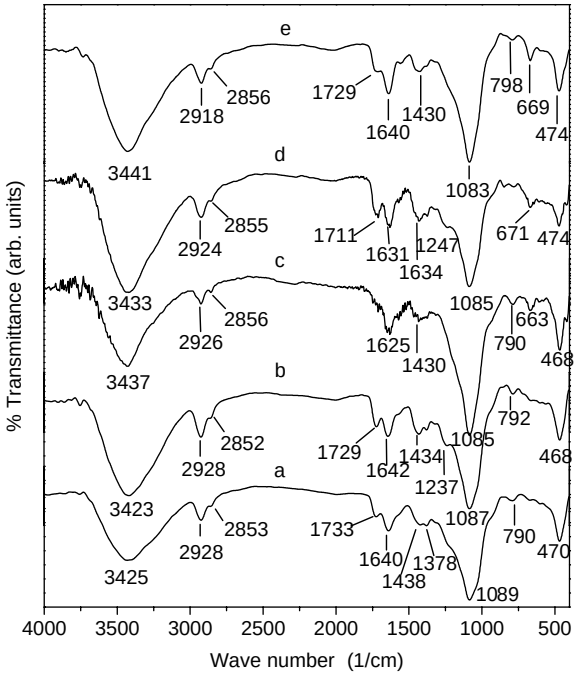

Fig. 1. FTIR spectrums of (a) pure PVA, (b) 1 wt%, (c) 5 wt%, (d) 10 wt%, and (e) 20 wt% $BaCl_2$ doped PVA samples.

are at 1438 and 1378 cm^{-1}, respectively, and C–H wagging at 1247 cm^{-1} [7,11,12].

In the case of $BaCl_2$ doped PVA, the FTIR spectra shows shifts in the corresponding bands with a change in intensities. This indicates the considerable interaction between PVA and $BaCl_2$. From the figure it is clear that the stretching frequencies of acetyl C=O of PVA shifts from 1640 to 1642 (1 wt%), 1625 (5 wt%), 1631 cm^{-1} (10 wt%) and for 20 wt% original stretching band reappears at 1640 cm^{-1}. These observations suggest that only at low dopant concentrations the interaction between barium ions with acetyl group dominates (as given in the Scheme 1). As the dopant concentration increases, these interactions results in the formation of dopant aggregates or agglomerates leading to a certain phase separation into a polymer-rich phase and a dopant-rich phase. Hence, the reappearance of 1640 cm^{-1} band for 20 wt% dopant concentration may be due to polymer rich phase.

The stretching frequency of C=C shifts from 1733 to 1729, 1711 cm^{-1}, respectively. The shift in bending of CH_2 vibrations are from 1438 to 1434, 1430 cm^{-1} indicates the chemical interactions of Ba^{2+} ions with PVA matrix. The shift in acetyle C–O stretching of PVA with a sharp decrease in the peak intensity is from 1089 to 1087, 1085, and 1083 cm^{-1} also supports the existence of chemical interaction. This modification may be understood by invoking to the intra/inter molecular hydrogen bonding and complex formation of the PVA molecules with the $BaCl_2$ as shown in the Scheme 1 below Thus, it can be concluded that the OH group of the PVA interact with Ba^{2+} ions of $BaCl_2$ form a complex. Due to this interaction and complex formation, the frequencies corresponding to other vibrations in PVA such as $–CH_2$, –CH group and C–O groups will be affected which is reflected in the Fig. 1. It also modifies the wagging, bending, skeletal and out of plane vibrations.

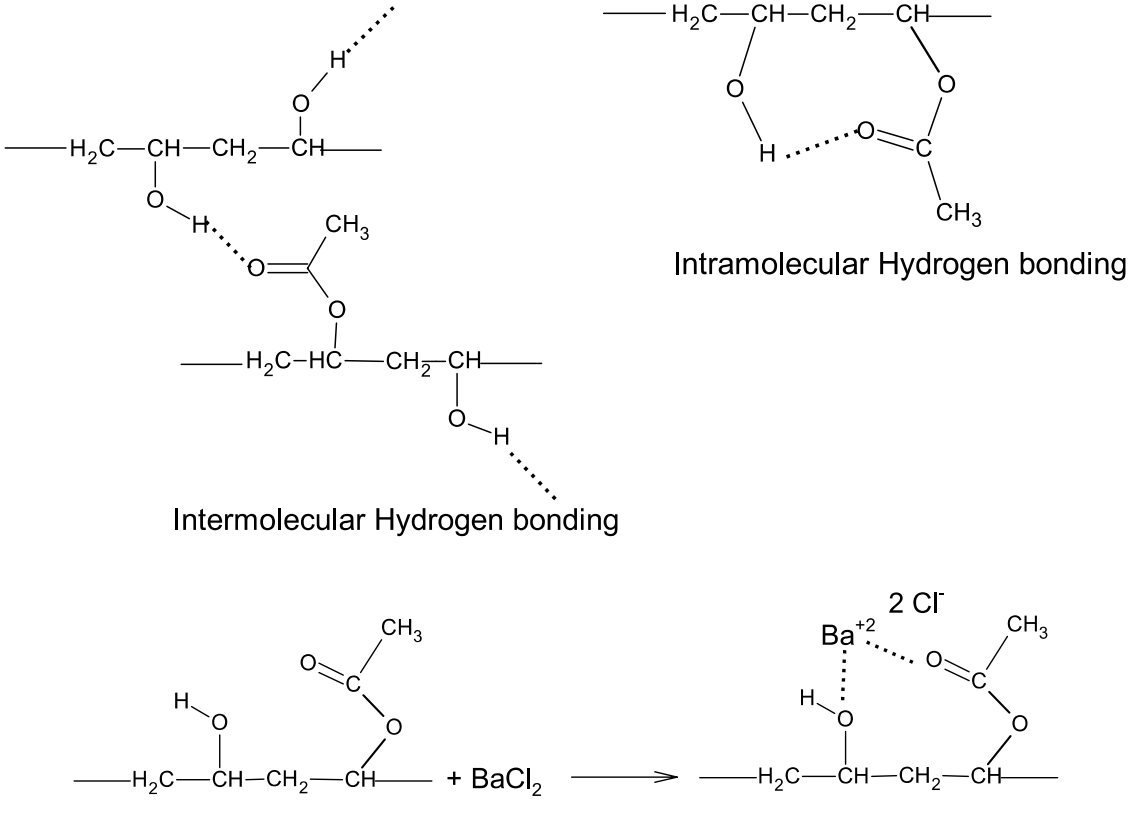

Scheme 1.

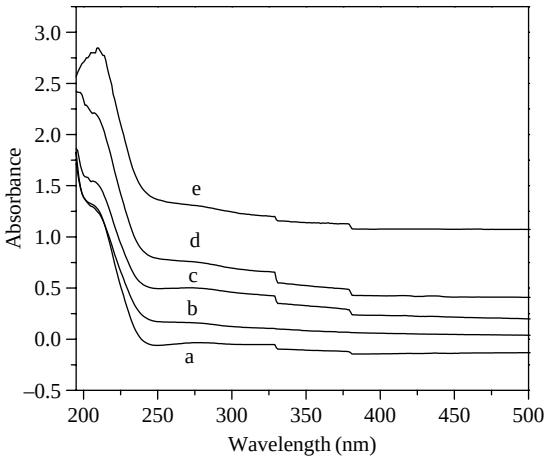

Fig. 2. UV–visible spectra of (a) pure PVA, (b) 1 wt%, (c) 5 wt%, (d) 10 wt%, and (e) 20 wt% $BaCl_2$ doped PVA samples.

3.2. UV–visible studies

The UV–visible absorption spectra of pure as well as $BaCl_2$ doped PVA are shown in the Fig. 2. The observed results like the absorption band, absorption edges and band assignments are given in Table 1. The absorption band at 196 nm in PVA was assign to n–π* transitions and around 208 nm indicates the presence of unsaturated bonds, C=O and/or C=C mainly in the tail–head of the polymer PVA. The absorption band at 281 nm was assigned to π–π* transition. The sharp absorption edge around 245 nm in pure PVA indicates the semi crystalline nature of PVA. As expected, the PVA contains single bonds in the main chain and double bonds in the branches; the observed absorption in the UV (195–300 nm) region is understood [13].

The Fig. 2 shows, a shift in both absorption bands and band edges towards the higher wavelengths with different absorption intensity for the doped PVA. These shifts in the bands indicate the formation of inter/intra molecular hydrogen bonding mainly between Ba^{2+} ions with the adjacent OH groups that are in consistence with FTIR results. As the $BaCl_2$ concentration increases, inter/intra hydrogen bonding increases and hence absorption. This is in accordance with the Beer's law, i.e. the absorption is proportional to the number of absorbing molecules. The shift in absorption edge in the doped PVA reflects the variation in the energy band gap, which arises due to the variation in crystallinity with in the polymer matrix.

Table 1
Optical absorption data of pure and $BaCl_2$ doped PVA

Sample (wt%) (PVA + $BaCl_2$)	λ_{max} (nm)	Assignment	λ_{edg} (nm)
0	196	n → π*	245
	208	π → π*	
	281	π → π*	
1	196	n → π*	253
	209	π → π*	
	275	π → π*	
5	199	n → π*	261
	209	π → π*	
	277	π → π*	
10	198	n → π*	263
	208	π → π*	
	280	π → π*	
20	210	π → π*	272
	276	π → π*	

3.3. Determination of the optical energy band gap E_g

It is well known that the relationship between the absorption coefficient α and the optical band gap E_g, obeys the classical Tauc's expression. Using the observed UV–visible spectra, the optical energy band gap is determined by translating the spectra into Tauc's plots. To translate the absorption spectrum in to Tauc's plot, we use the frequency dependent absorption coefficient given by Mott and Devis [2,14,15]

$$\alpha(v) = \frac{\beta(h\nu - E_g)^r}{h\nu}$$

where β is a constant and the exponent r is an empirical index, which is equal to 2 for indirect allowed transition in the quantum mechanical sense, responsible for optical absorption.

The plot of the product of absorption coefficient and photon energy $(\alpha h\nu)^{1/2}$ verses the photon energy $h\nu$ at room temperature shows a linear behavior, which can be considered as an evidence for indirect allowed transition. Extrapolation of the linear portion of this curve to a point $(\alpha h\nu)^{1/2} = 0$ gives the optical energy band gap E_g for the pure as well as doped PVA films (Fig. 3). Here, the transition between the valence and conduction bands is assumed to be an allowed indirect transition. The calculated E_g for all the samples and its variations are given in Fig. 4. The figure shows that the band gap decreases with increase in dopant concentration.

The existence and variation of optical energy gap E_g may be explained by invoking the occurrence of local cross linking within the amorphous phase of the polymer, in such a way as to increase the degree of ordering in these parts [5]. As observed in FTIR studies, Ba^{2+} ion of $BaCl_2$ interacts with –OH group of PVA and forms complex in the form of intra/inter molecular hydrogen bonding. These interaction and hence the complex

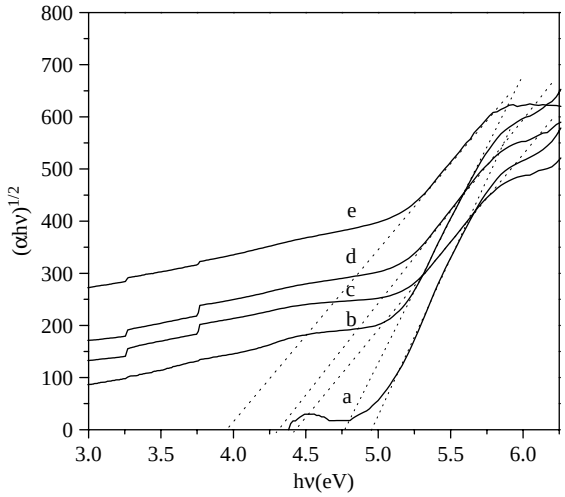

Fig. 3. Optical energy band gap of (a) pure PVA, (b) 1 wt%, (c) 5 wt%, (d) 10 wt%, and (e) 20 wt% $BaCl_2$ doped PVA samples.

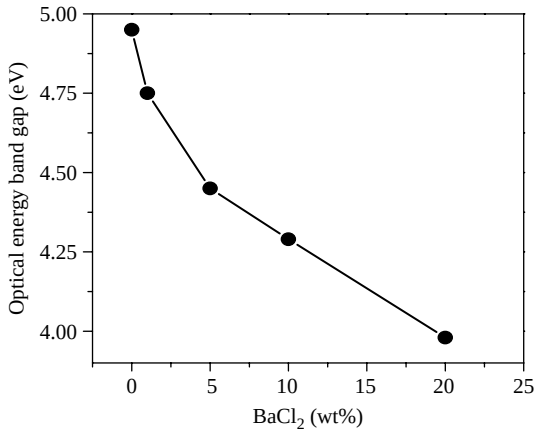

Fig. 4. Variation of the optical energy band gap of the pure and $BaCl_2$ doped PVA.

formation causes the microstructural variation within the polymer matrix. This microstructural variation increases with dopant concentration, which is reflected in the form of decrease in the energy band gap E_g (Fig. 4).

3.4. XRD studies

The microstructural variations of PVA upon the incorporation of $BaCl_2$ salt are investigated using Wide angle X-ray diffractogram (WAXD). The observed WAXD for pure as well as $BaCl_2$ doped PVA films are shown in the Fig. 5. The figure shows a relatively sharp and broad peak centered on $2\theta = 19.56°$ ($d = 4.5347$ Å) indicates the semicrystalline nature of the polymer PVA contains crystalline and amorphous regions.

The crystalline phase of this polymer may be regarded as an amorphous matrix in which small crystallites are randomly distributed. However, it is more natural to treat a crystalline region as a certain sufficiently imperfect crystalline lattice in which free volumes are filled with amorphous phase. Sites saturated with crystal defects, which are due to chain-folded crystals, may play the role of amorphous regions [16].

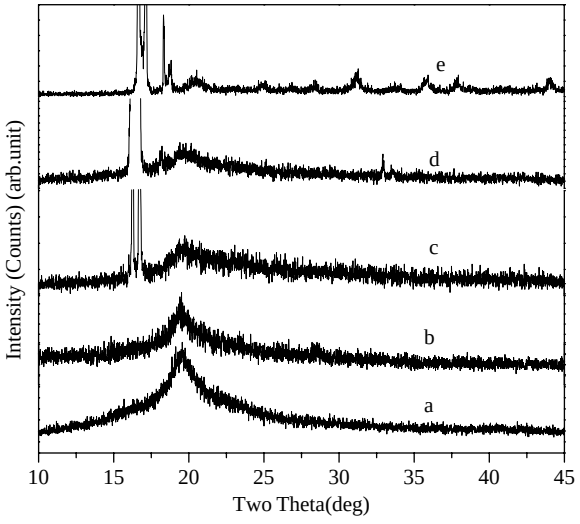

Fig. 5. X-ray diffractograms of (a) pure PVA, (b) 1 wt%, (c) 5 wt%, (d) 10 wt%, and (e) 20 wt% $BaCl_2$ doped PVA samples.

In the case of $BaCl_2$ doped PVA, we observe various sharp peaks as shown in the Fig. 5 except for 1 wt%. The unchanged nature of a broad peak at $2\theta = 19.51°$ ($d = 4.5462$ Å) for 1 wt% of $BaCl_2$ indicates that the crystallinity will remains the same as that of pure PVA. After 5 wt% of $BaCl_2$ we observed many multiple peaks with respect to main peak, which are presented in Table 2. The behavior of the crystallinity is also expressed in terms of relative intensities (I/I_0) of the crystalline peaks. These relative intensities of the peaks are obtained by X-ray data using PowderX Software. Here, I is the intensity in counts at any peak, I_0 is the intensity of the prominent peak and I/I_0 is the percentage relative intensity.

From these data one can notice that, at small angles, the first order diffraction shifts to lower angles compared with pure PVA. The amorphous broad band is decreased and appearance of sharp peaks starts for 5 wt% doped samples on wards. These results also show clearly that the dopant interacts with the polymer chain mainly with the hydroxyl group as observed in FTIR spectra, and increases the crystallinity with dopant. The increase in crystalline phase of the semicrystalline PVA matrix with the doping of $BaCl_2$ is the result of the local ordering in the polymeric structure due to complex formation. Here, the Ba^{2+} ions may occupy the interstitial sites between the polymer chains of amorphous phase and link them with hydrogen bond due to charge transport processes. These crystalline regions are connected to amorphous regions in which the molecular chains of the polymer are irregularly folded. This interaction of hydroxyl groups present in the side chain with the barium ions has a significant influence on the polymer chain mobility and on the structure.

In order to study these variations, the average crystallite sizes P are estimated using the observed WAXD data for pure as well as $BaCl_2$ doped PVA films with Scherrer's equation [16]

$$P = \frac{k\lambda}{(\beta \cos \theta)}$$

Table 2
WXRD results of pure and $BaCl_2$ doped PVA

Sample (wt%) (PVA + $BaCl_2$)	2θ	d-spacing (Å)	I/I_0	Crystallinity (%)	P (nm)	R (Å)
0	19.56	4.5347	100	56	2.92	5.66
1	19.51	4.5462	100	62	5.20	5.68
5	16.25	5.4488	100	69	85.28	6.77
	16.72	5.2966	82.42			
	19.35	4.5815	11.41			
	19.72	4.4975	12.20			
	20.61	4.3060	9.76			
10	16.33	5.4209	100	85	87.55	6.65
	16.43	5.3892	62.68			
20	16.62	5.3282	100	90	94.18	6.81
	17.14	5.1680	47.41			
	18.31	4.8405	12.42			

where $k=0.9$ or 1 is a constant and related to several aspects including the shape of the crystal and the Miller index of the reflecting crystallographic planes and crystallite shape, β is width at half maximum intensity of the reflection in radians, θ is the Bragg's angle, $\lambda=1.5405$ Å is the wavelength of the X-ray radiation. The results of the calculated crystallite size are tabulated in the Table 2. From the table it is clear that the width at half maximum intensity β decreased with an increasing amount of $BaCl_2$ and hence the crystallites size increases sharply with dopant concentration. This indicates that the crystallites of PVA were highly ordered in the doped PVA films than in the pure PVA, which reflects the microstructural variations with in the doped PVA. At 20 wt% concentrations onwards the existence of two or more crystalline phases within the polymer may not be ruled out. In this case, the first crystalline phase may be the main phase of PVA and second phase characterized due to the PVA–Ba^{2+} complex, may be because the Ba^{2+} ion (ionic radius $\sim$1.35 Å) is too large to fit into the crystalline structure of PVA.

The average inter crystallite separation (R) in the amorphous region of the sample was evaluated from the position of the maximum of the halo [17]

$$R = \frac{5\lambda}{8 \sin \theta}$$

From the above equation the calculated distance between the hydroxyl groups of crystalline PVA is 5.668 Å. The average inter-crystallite separation in $BaCl_2$ doped PVA films are shown in the Table 2.

3.5. DSC studies

The thermal behavior of the $BaCl_2$ doped PVA was studied using DSC from room temperature to 195 °C and the observed thermograms are shown in the Fig. 6. The figure shows two endothermic peaks for pure PVA and multiple peaks for doped PVA.

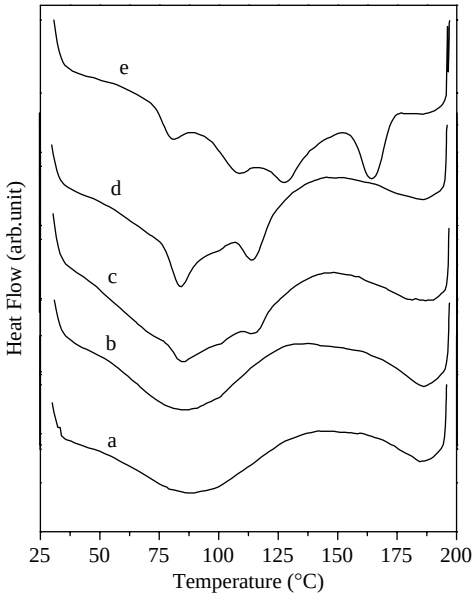

Fig. 6. DSC thermograms of (a) pure PVA, (b) 1 wt%, (c) 5 wt%, (d) 10 wt%, and (e) 20 wt% $BaCl_2$ doped PVA samples.

Using the thermograms, the observed first transition around 60–75 °C was attributed to the glass transition temperature (T_g) of the relaxation process resulting from micro-Brownian motion of the main chain backbone. This T_g is calculated by taking the mid point of the first endothermic peak during heating. It is a known fact that below T_g, molecules do not have segmental motion, and some portions of the molecules may not wiggle around, but may only be able to vibrate slightly. Near T_g, the molecules can start vibrating and segmental motion increases. The conformational changes, i.e. changes in molecular shape, are caused either by thermal motion or by the action of an external field without rupture of chemical bonds. Accordingly the transition at 88–81 °C for all samples were attributed to the α-relaxation (T_α) associated with the crystalline region. The broad endothermic peaks around 184–186 °C for pure as well as 1 wt% $BaCl_2$ were assigned to the melting temperature T_m, which indicates the semicrystalline nature of the PVA. Fig. 6 shows multiple peaks between T_α and T_m, with decrease in T_g for $BaCl_2$ doped PVA as compared to pure PVA. Many researchers have observed similar type of results for other systems [8–10,16,17].

The Fig. 6 shows that the position of T_g and T_α for PVA films filled with different amounts of $BaCl_2$ was shifted slightly toward lower temperatures with respect to the unfilled film (Table 3), suggests the reduction in the thermal stability. This shows that the segmental mobility of amorphous PVA increased with the addition of $BaCl_2$ and the PVA segments became less rigid. This indicate the $BaCl_2$ dopant acts as plasticizer in PVA, therefore, the $BaCl_2$ molecules greatly affected the PVA structure.

Fig. 7 shows the variation of T_g and T_α with $BaCl_2$ concentration. From the figure, the shift in T_α might be due to the effect of doping on the orientation of the crystals, crystallinity, and microstructure of the sample. It is known that the changes in the crystalline structure and morphology affect the magnitude and position of the α-relaxation process in PVA. Hence, it is expected, T_α could be influenced by the size and perfection of the crystals and, therefore, their T_m values. From the figure, the magnitude and shift in T_α of the relaxation have been affected by the orientation of the crystals, the crystallinity and microstructure of the sample.

If the α-relaxation in PVA were associated with a particular movement, its intensity would have varied with the crystal orientation. Therefore, the decrease in magnitude of the

Table 3
DSC results of pure and $BaCl_2$ doped PVA

Samples (PVA+ $BaCl_2$)	T_g (°C)	T_α (°C)	T_{m1} (°C)	T_{m2} (°C)	T_{m3} (°C)	T_{m4} (°C)
0	65	88	185	–	–	–
1	64	85	186	–	–	–
5	62	85	187	113	–	–
10	60	84	188	114	101	–
20	58	81	190	164	128	109

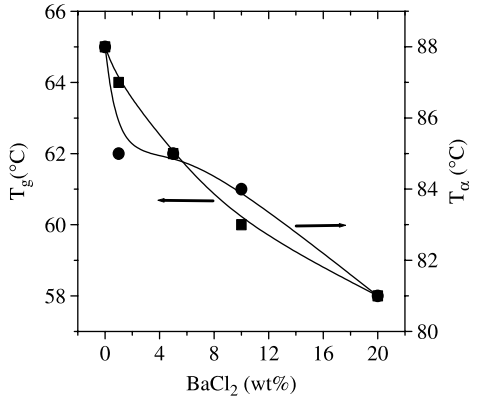

Fig. 7. Variation of glass transition temperature T_g and T_α with $BaCl_2$ concentration.

transition suggests that the motions were perpendicular to the chain axis, which means the orientation of the crystals along the chain axis increases. Also, the α-relaxation magnitude depended on the density and perfection of the crystal packing and depended on the crystal thickness.

Following Kissinger's formula [5], which is valid for the crystallization process, the glass transition temperature T_g is related to the steady heating rate ψ by

$$\log\left(\frac{T_g^2}{\psi}\right) + \text{const} = \frac{E_g}{4.58T_g}$$

where E_g is the apparent activation energy of glass transition, ψ in the present case is 10°/min. The plot of the relationship between $\log(T_g^2/\psi)$ and $1/T_g$ is a linear curve for the studied samples as can be seen in the Fig. 8. Using this graph E_g the activation energy is found to be 15.45006 kJ/mol.

The observed multiple peaks, whose number increases with concentration, in addition to increase in T_m may be attributed to the increase in the crystallite thickness in the crystalline phase formed during the filling of $BaCl_2$. This indicates that the increase in size of the crystallite and/or the order of the molecular packing in the crystallites with the $BaCl_2$ content. Similar behavior is also reflected in the XRD study (Fig. 5),

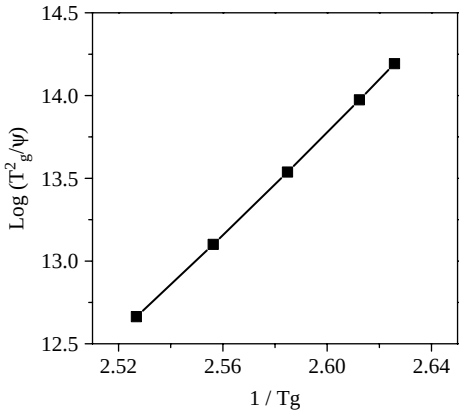

Fig. 8. Variations of $\log(T_g^2/\psi)$ with $1/T_g$ for $BaCl_2$ doped PVA.

where in the appearance of sharp peaks increases for PVA films filled with $BaCl_2$. This implied that the crystalline phase changed with increasing dopant content.

The formation of the crystalline phase in the amorphous PVA matrix with the filling of $BaCl_2$ was interpreted as follows. The addition of $BaCl_2$ to the PVA causes a tendency to local ordering in the polymeric structure. This local ordering might have been accomplished by intramolecular and intermolecular interactions in the polymer structure.

The origin of two or more T_ms in the DSC scans for $BaCl_2$ more than 10 wt% supports the existence of two crystalline phases. The first crystalline phase may be the main phase of PVA, which decreased with increasing $BaCl_2$ content because of the induced defects, and the second crystalline phase characterized the PVA–Ba^{2+} complex. This complex arises due to increase in inter/intra molecular interactions as explained in FTIR study. At higher dopant concentration the formation of dopant aggregates or agglomerates leading to a certain phase separation into a polymer-rich phase and a dopant-rich phase or increase in crystallinity may not be ruled out.

4. Conclusions

We have studied the effect of $BaCl_2$ on the optical, thermal and structural properties of a semicrystalline polymer PVA. The FTIR study shows that the Ba^{2+} ions of dopant $BaCl_2$ interacts with the OH groups of PVA and forms a complex via intra/inter molecular hydrogen bonding. The UV–visible optical studies also reflect the complex formation and its effect on the microstructure. These microstructural changes due to complex formation is reflects in the form of variation in the band gap as well as the other optical properties. The XRD results show that, due to the interaction of dopant and hence the complex formation, the structural repositioning takes place, which increases the crystallinity. The DSC studies indicate that the dopant changes the thermal behavior of PVA like glass transition temperature and dopant acts as a plasticizer. This also suggests that the interaction of dopant and PVA molecule changes the crystallite parameters and the degree of crystallinity, which supports the XRD results. At higher dopant concentrations the formation of phase separation into a polymer-rich phase and a dopant-rich phase or increase in crystallinity can also expected.

Acknowledgements

The authors are thankful to The Director, Microtron Center, The Research Coordinator, OSTC and The Chairman, Department of Materials Science, Mangalore University for providing the experimental facilities for this work. The authors are also thankful to Dr. Cheng Dong, Institute of Physics, Chinese Academy of Sciences, Beijing, P.R. China for PowderX software. Two of us (RFB and AH) are greateful to UGC, Govt of India for awarding FIP Fellowship.

References

[1] Bulinski M, Kuncser V, Plapcianu C, Krautwald S, Franke H, Rotaru P, et al. J Phys D: Appl Phys 2004;37:2437–41.
[2] Zidan HM. J Appl Polym Sci 2003;88:104–11.
[3] Lobo B, Ranganath MR, Ravi Chandran TSG, Venugopal Rao G, Ravindrachary V, Gopal S. Phys Rev B 1999;59:13693.
[4] De-Huang W. Thin Solid Films 1996;288:254–5.
[5] AEl-Shahawy M. Polym Int 2003;52:1919–24.
[6] Tawansi A, El-Khodary A, Abdelnaby MM. Curr Appl Phys 2005;5:572–8.
[7] Soliman Selim M, Seoudi R, Shabaka AA. Mater Lett 2005;59:2650–4.
[8] Yasuniwa M, Tsubakihara S, Fujioka T. Thermochim Acta 2003;396: 75–8.
[9] Wei C-L, Chen M, Yu F-E. Polymer 2003;44:8185–93.
[10] Liu T, Petermann J. Polymer 2001;42:6453–61.
[11] Shin EJ, Lee YH, Choi SC. J Appl Polym Sci 2004;91:2407–15.
[12] Dai L, Li J, Yamada E. J Appl Polym Sci 2002;86:2342–7.
[13] Abd El-Kader KAM, Abdel Hamied SF. J Appl Polym Sci 2002;86: 1219–26.
[14] Mott NF, Devis NF. Electronic process in non-crystalline materials. 2nd ed. Oxford: Oxford University Press; 1979 p. 273.
[15] Tauc J. In: Abeles F, editor. Optical properties of solid. Amsterdam: North-Holland; 1972. p. 277–313.
[16] Zidan HM. J Appl Polym Sci 2003;88:1115–20.
[17] Kundu PP, Biswas J, Kim H, Choe S. Eur Polym J 2003;39: 1585–93.